SPATIAL-VECTOR SMOOTHING FOR COHERENT SOURCES IN PRESENCE OF A REFLECTING BOUNDARY

Jianwu TAO

Department of Electrical and Computer Engineering, University of Waterloo, Waterloo, Ontario, N2L 3G1, Canada

ABSTRACT

A new spatial-vector smoothing algorithm for $multiple$ coherent sources is proposed based on the measurement model of 3-D cylindrical array with multi vector-hydrophones, which is located on or near a reflecting boundary. And the performance of the proposed algorithm is examined in two practical applications: hull-mounted and seabed array. The advantages of the spatial-vector smoothing scheme are: (1) less reduction in the overall array's spatial aperture, (2) no limit to the maximum number of coherent sources.

1. INTRODUCTION

A vector-hydrophone consists of either two or three identical but orthogonally oriented velocity hydrophones plus a pressure hydrophone, all of which are spatially co-located in a point-like geometry. The four-component vector-hydrophone produces the following 4×1 array manifold with regard to the k-th source impinging from elevation angle $0 \leq \theta_k < \pi$ (measured from the vertical z-axis) and azimuth angle $0 \leq \phi_k < 2\pi$ [1]:

$$\mathbf{H}(\theta_k, \phi_k) \stackrel{\text{def}}{=} \begin{bmatrix} u(\theta_k, \phi_k) \\ v(\theta_k, \phi_k) \\ w(\theta_k) \\ 1 \end{bmatrix} = \begin{bmatrix} \sin\theta_k \cos\phi_k \\ \sin\theta_k \sin\phi_k \\ \cos\theta_k \\ 1 \end{bmatrix} \qquad (1)$$

In many practical applications, an array of vector-hydrophones is located on or near a reflecting boundary. For example, a cylindrical array with vector hydrophones is mounted on an submarine hulls [2]; or it is mounted on the sea bed in shallow water. The measurement model of array with multiple vector-sensors for $single$ source, where all vector-sensors lie on a 2-D plane near a reflecting boundary, have been proposed in [3], and based on this model, the performance to estimate the DOA of single source is examined. For multiple coherent sources, however, the restoring rank problem is not considered in [3].

In order to exploit based-subspace techniques to estimate the DOA of coherent signals, the preprocessing methods are first need to restore the rank of covariance matrix of incident signals. The early preprocessing scheme referred to as $spatial\ smoothing$ was proposed in [4],[5],[6]. The spatial smoothing technique, however, suffer from the reduction of the effective array aperture due to dividing an array into some subarray, resulting in lower resolution and accuracy. Another approach referred to as $vector\ smoothing$ was proposed in [7]. But, the disadvantage of vector smoothing technique is that the maximum number of restoring the rank of covariance matrix of coherent sources is limited since the component-number of vector sensor is a constant. For example, the vector smoothing technique can only restore the rank of covariance matrix of coherent sources up to 4 for an array with four-component vector-hydrophones.

In this paper, a new spatial-vector smoothing algorithms for $multiple$ coherent sources is proposed based on the measurement model of 3-D cylindrical array with multi vector-hydrophones, which is located on or near a reflecting boundary. And the performance of the proposed algorithm is examined in two practical applications: hull-mounted and seabed array. The advantages of the proposed smoothing scheme are: (1) less reduction in the overall array's spatial aperture, (2) no limit to the maximum number of coherent sources.

2. THE MODEL OF A CYLINDRICAL VECTOR-HYDROPHONE ARRAY

Consider a uniform cylindrical array with L ($L = P \times M$) vector-hydrophones, P number of circular rings of radius R all centered around the vertical z-axis and mutually separated by D vertically. M vector-hydrophones are uniformly placed on circular at $2\pi/M$ adjacent apart. For the (p, m)th vector-hydrophone located at x_m, y_m, z_p has spatial phase factor

$$q_{p,m}(\theta_k, \phi_k) = e^{j2\pi(x_m u(\theta_k,\phi_k) + y_m v(\theta_k,\phi_k) + z_p w(\theta_k))/\lambda} \qquad (2)$$

where $x_m = R{*}cos(2\pi(m-1)/M)$, $y_m = R{*}sin(2\pi(m-1)/M)$, $z_p = D(p-1)$, $\forall\ 1 \leq p \leq P, \forall\ 1 \leq m \leq M$. The $u(\theta_k, \phi_k), v(\theta_k, \phi_k), w(\theta_k)$ are the kth source direction cosines, along the x-axis, y-axis and z-axis, respectively. λ denotes the wavelength of incidence wave. Let

$$\mathbf{q}^{(p)}(\theta_k, \phi_k) = \begin{bmatrix} q_{p,1}(\theta_k, \phi_k) \\ \vdots \\ q_{p,M}(\theta_k, \phi_k) \end{bmatrix} \quad p = 1, \ldots, P \ (3)$$

Assuming the first circular ring of cylindrical array ($p = 1$) located on the plane $z = 0$, the boundary lies in the $z = -d$ plane, and oriented such that its velocity sensors measure the velocity components parallel to the coordinate axes. K ($K < L$) narrowband, far-field underwater acoustic planewave impinge upon the cylindrical array. The $4L \times 1$ vector measurements $\mathbf{z}(t)$ at time t:

$$\mathbf{z}(t) = \sum_{k=1}^{K} \mathbf{a}(\theta_k, \phi_k)\tilde{p}_k(t) + \mathbf{n}(t) = \mathbf{A}\tilde{\mathbf{p}}(t) + \mathbf{n}(t) \quad (4)$$

for $t = 1, 2, \cdots, N$, $\tilde{\mathbf{p}}(t) \stackrel{\text{def}}{=} [\tilde{p}_1(t), \cdots, \tilde{p}_K(t)]^T$ is the complex amplitude vector of the incident wave. $\mathbf{n}(t)$ is the additive noise vector. $\mathbf{A} \stackrel{\text{def}}{=} [\mathbf{a}(\theta_1, \phi_1), \cdots, \mathbf{a}(\theta_K, \phi_K)]$ is the direction matrix of cylindrical array. $\mathbf{a}(\theta_k, \phi_k)$ is the steering vector, i.e.

$$\mathbf{a}(\theta_k, \phi_k) = \begin{bmatrix} \mathbf{q}^{(1)}(\theta_k, \phi_k) \otimes \mathbf{h}^{(1)}(\theta_k, \phi_k) \\ \vdots \\ \mathbf{q}^{(P)}(\theta_k, \phi_k) \otimes \mathbf{h}^{(P)}(\theta_k, \phi_k) \end{bmatrix} \quad (5)$$

where $\otimes$ is the Kronecker product.

$$\mathbf{h}^{(p)}(\theta_k, \phi_k) = \begin{bmatrix} (1 + \mathcal{R}(\theta_k)e^{-i\vartheta_k^{(p)}})u(\theta_k, \phi_k) \\ (1 + \mathcal{R}(\theta_k)e^{-i\vartheta_k^{(p)}})v(\theta_k, \phi_k) \\ (1 - \mathcal{R}(\theta_k)e^{-i\vartheta_k^{(p)}})w(\theta_k) \\ (1 + \mathcal{R}(\theta_k)e^{-i\vartheta_k^{(p)}}) \end{bmatrix} \quad (6)$$

where $\vartheta_k^{(p)} = 4\pi((p-1)D + d)\sin\theta_k/\lambda$, $p = 1, \ldots, P$, $\mathcal{R}$ is the (complex) reflection coefficient, which specifies the attenuation and phase change of the reflected wave. By our choice of coordinate system, the incident angle γ is just $\pi/2 - \theta$; therefore, for a given frequency, $\mathcal{R}$ is a function of θ but not ϕ.

3. THE SPATIAL-VECTOR SMOOTHING(SVS)

Supposing that K narrowband underwater acoustic sources are coherent, i.e. $\tilde{\mathbf{p}}(t) = [g_1, \cdots, g_K]^T \tilde{p}_1(t) = \mathbf{g}\tilde{p}_1(t)$ (g_k is a complex constant), the $4M \times K$ array manifold $\mathbf{A}^{(p)}$ of the pth circular ring may be partitioned into 4 number of $M \times K$ subarray manifolds, i.e.

$$\mathbf{A}_j^{(p)} = \mathbf{Q}^{(p)}\mathbf{\Phi}_j^{(p)}, \quad j = 1, \ldots, 4 \quad (7)$$

$$\mathbf{Q}^{(p)} \stackrel{\text{def}}{=} \left[\mathbf{q}^{(p)}(\theta_1, \phi_1), \cdots, \mathbf{q}^{(p)}(\theta_K, \phi_K)\right] \quad (8)$$

where $\mathbf{\Phi}_j^{(p)}$ is a diagonal matrix, its diagonal elements are

$$\left[\mathbf{\Phi}_j^{(p)}\right]_{k,k} = \begin{cases} (1 + \mathcal{R}(\theta_k)e^{-i\vartheta_k^{(p)}})u(\theta_k, \phi_k), & \text{j} = 1 \\ (1 + \mathcal{R}(\theta_k)e^{-i\vartheta_k^{(p)}})v(\theta_k, \phi_k), & \text{j} = 2 \\ (1 - \mathcal{R}(\theta_k)e^{-i\vartheta_k^{(p)}})w(\theta_k), & \text{j} = 3 \\ (1 + \mathcal{R}(\theta_k)e^{-i\vartheta_k^{(p)}}), & \text{j} = 4 \end{cases} \quad (9)$$

None of them depends on $\{(x_m, y_m), m = 1, \ldots, M\}$. And $\mathbf{Q}^{(p)} = \mathbf{Q}^{(1)}\mathbf{\Psi}^{(p-1)}$, where $\mathbf{\Psi}^{(p-1)}$ is a diagonal matrix with diagonal elements $\{[\mathbf{\Psi}^{(p-1)}]_{k,k} = e^{i2\pi D(p-1)w(\theta_k)/\lambda}$, $k = 1, \ldots, K\}$.

The sample covariances matrix of outputs of 4 subarrays are averaged,

$$\bar{\mathbf{R}}^{(p)} = \frac{1}{4}\sum_{j=1}^{4} \mathbf{R}_j^{(p)} = \mathbf{Q}^{(p)}\bar{\mathbf{R}}_{\tilde{p}}^{(p)}(\mathbf{Q}^{(p)})^H + \bar{\mathbf{R}}_n^{(p)} \quad (10)$$

$$\begin{aligned} \bar{\mathbf{R}}_{\tilde{p}}^{(p)} &= \frac{1}{4}\sum_{j=1}^{4} \mathbf{\Phi}_j^{(p)}\mathbf{R}_{\tilde{p}}(\mathbf{\Phi}_j^{(p)})^H \\ &= \frac{\mathcal{P}_1}{4}\sum_{j=1}^{4} \mathbf{\Phi}_j^{(p)}\mathbf{g}\mathbf{g}^H(\mathbf{\Phi}_j^{(p)})^H \\ &= \frac{\mathcal{P}_1}{4}(\mathbf{G}\mathbf{D}^{(p)})(\mathbf{G}\mathbf{D}^{(p)})^H \end{aligned} \quad (11)$$

where $\mathcal{P}_1 \stackrel{\text{def}}{=} \frac{1}{N}\sum_{t=1}^{N} \tilde{p}_1(t)\tilde{p}_1^*(t)$, $\mathbf{G} \stackrel{\text{def}}{=} diag\{g_1, \cdots, g_K\}$ is a diagonal matrix.

$$\mathbf{D}^{(p)} = \begin{bmatrix} u(\theta_1, \phi_1) & v(\theta_1, \phi_1) & w(\theta_1) & 1 \\ \vdots & \vdots & \vdots & \vdots \\ u(\theta_K, \phi_K) & v(\theta_K, \phi_K) & w(\theta_K) & 1 \end{bmatrix} \odot \begin{bmatrix} \mathbf{h}^{(p)}(\theta_1, \phi_1) & \cdots & \mathbf{h}^{(p)}(\theta_K, \phi_K) \end{bmatrix}^T \quad (12)$$

where $\odot$ is indicates the element-wise product. $p = 1, \ldots, P$.

Then, smoothed covariance matrix $\bar{\mathbf{R}}^{(p)}$ of P circular ring are again averaged,

$$\bar{\mathbf{R}} = \frac{1}{P}\sum_{p=1}^{P} \bar{\mathbf{R}}^{(p)} = \mathbf{Q}^{(1)}\bar{\mathbf{R}}_{\tilde{p}}(\mathbf{Q}^{(1)})^H + \bar{\mathbf{R}}_n \quad (13)$$

$$\begin{aligned} \bar{\mathbf{R}}_{\tilde{p}} &= \frac{1}{P}\sum_{p=1}^{P} \mathbf{\Psi}^{(p-1)}\bar{\mathbf{R}}_{\tilde{p}}^{(p)}(\mathbf{\Psi}^{(p-1)})^H \\ &= \frac{\mathcal{P}_1}{4P}(\mathbf{G}\mathbf{\Theta})(\mathbf{G}\mathbf{\Theta})^H \end{aligned} \quad (14)$$

where

$$\mathbf{\Theta} = \begin{bmatrix} \mathbf{D}^{(1)}, & \mathbf{\Psi}^{(1)}\mathbf{D}^{(2)}, & \cdots, & \mathbf{\Psi}^{(P-1)}\mathbf{D}^{(P)} \end{bmatrix} \quad (15)$$

Since rank$\{\mathbf{G}\} = K$, rank$\{\bar{\mathbf{R}}_{\tilde{p}}\}$ =rank$\{\mathbf{\Theta}\}$. When $\theta_i \neq \theta_j$, $\phi_i \neq \phi_j$ at $\forall i \neq j$, and $|\mathcal{R}(\theta_i)| \neq 0$, $\vartheta_i + \angle\mathcal{R}(\theta_i) \neq n\pi$ at $i = 1, \ldots, K$ (where $\mathcal{R}(\theta_i) = |\mathcal{R}(\theta_i)|e^{\angle\mathcal{R}(\theta_i)}$, n is an integer), rank$\{\mathbf{\Theta}\}$ = Min$\{K, 4P\}$ is clearly obtained form (12) and (15).

It is noted that the SVS is not limited to 3-D cylindrical array. It may easy extended to other center array (see definition in [6]) with an ambiguity-free structure. The SVS for the usual pressure-hydrophone array is a special case of this algorithm obtained by setting $\mathbf{h}^{(p)}(\theta_k, \phi_k) = [0, 0, 0, (1 + \mathcal{R}(\theta_k)e^{-i\vartheta_k^{(p)}})]$. In the case, vector smoothing will disappear.

The advantages of SVS are no reduction in the circular ring subarray's spatial aperture and no limit to the maximum number of the coherent sources.

4. THE PERFORMANCE OF SPATIAL-VECTOR SMOOTHING ALGORITHM

The $\mathcal{R}$ is a function of both incident wave's angle frequency and incidence angle, and it is highly dependent on the nature of both half spaces. Several ideal situations of practical applications will be discussed to examine the performance of the proposed smoothing algorithm.

4.1. Rigid Boundary

In case of $\mathcal{R} = 1$ for all incidence angles, such a surface is called a $rigid$ boundary, and is a good approximation to a vessel's hull at high frequency. Setting $\mathcal{R} = 1$ in (6), rank$\{\mathbf{\Theta}\}$ decreases to Min$\{K, 3P\}$ at $d = 0$ and $D = \lambda/2$ for all $\theta_i = \pi/2$ and $\phi_i \neq \phi_j$, because the normal velocity component is zero. To restore the rank to K (K coherent sources), $P \geq K/3$ is need. Whereas, if $d = \lambda/4$ and $D = \lambda/2$ for all $\theta_i = \pi/2$ and $\phi_i \neq \phi_j$, rank$\{\mathbf{\Theta}\}$ decreases Min$\{K, P\}$ because the pressure and in-plane velocity components are zero. To restore the rank to K, $P \geq K$ is need for. This is equivalent to a free space pressure-sensor array in rank restore. This means that $0 < d < \lambda/4$ should be selected to avoid rank lessen at $D = \lambda/2$.

4.2. Pressure-Release Boundary

In case of $\mathcal{R} = -1$ for all incidence angles, Such a surface is called a $pressure - release$ boundary, and is a approximation to a vessel's hull at low frequency. It is also a good approximation for underwater sound reflected from the interface with the air and is relevant to a floating or towed array scenario[3]. Setting $\mathcal{R} = -1$ in (6), the situation is the very reverse of $\mathcal{R} = 1$. If $d = \lambda/4$ and $D = \lambda/2$ for all $\theta_i = \pi/2$ and $\phi_i \neq \phi_j$, rank$\{\mathbf{\Theta}\}$ decreases Min$\{K, 3P\}$. If $d = 0$ and $D = \lambda/2$ for all $\theta_i = \pi/2$ and $\phi_i \neq \phi_j$, rank$\{\mathbf{\Theta}\}$ decreases Min$\{K, P\}$.

4.3. Seabed Model

The interface between sea water and the packed sandy ocean bottom can be approximately modeled the boundary between two fluids, one of which is absorptive. The reflection coefficient is given by [8]

$$\mathcal{R}(\gamma) \quad = \quad \frac{\eta \cos\gamma - i(\sin^2\gamma - n^2)^{1/2}}{\eta \cos\gamma + i(\sin^2\gamma - n^2)^{1/2}} \qquad (16)$$

where γ denotes the incident angle, η is the ratio of sand density to water density, and n is the index of refraction. The presence of absorption is expressed by assuming that the index of refraction is complex, i.e. $n = n_0(1+i\alpha)$, with $\alpha > 0$. For the sandy ocean bottom typical values are $n_0 = 0.83$, $\eta = 2.7$, $\alpha = 0.1$ [8]. Note that $\mathcal{R}$ does not depend on frequency in (16). Hence, all three components of velocity and pressure are generally nonzero at the surface. Thus, rank$\{\mathbf{\Theta}\}$ holds Min$\{K, 4P\}$ for $\theta_i \neq \theta_j$ and $\phi_i \neq \phi_j$.

5. NUMERICAL EXAMPLE

Supposing that two equal-power narrowband, coherent sources with $\theta_1 = 50°, \phi_1 = 40°, g_1 = 1, \theta_2 = 20°, \phi_2 = 70°, g_2 = e^{j\pi/6}$ impinge upon a cylindrical array with eight vector hydrophones, which consists of two 4-element uniformly circular rings with radius $R = \lambda/(2\sqrt{2})$ and inter-ring spacing D. The first circular ring of cylindrical array located on the plane $z = 0$, and the boundary lies in the $z = -d$ plane. The SNR is defined relative to each source. 100 snapshots are used in each of the 100 independent Monte Carlo trials.

As a overall error measure for the DOA estimation, the mean-square angular error (MSAE) for single source scenario is proposed, and a bound $\mathbf{MSAE}_B$ is derived on the MSAE in [9]. For K sources scenario, this bound may be expressed as

$$\mathbf{MSAE}_B = \frac{N}{K}\sum_{k=1}^{K}\{\cos^2\theta_k \cdot \mathbf{CRB}(\phi_k) + \mathbf{CRB}(\theta_k)\} \quad (17)$$

Fig. 1 shows the performance ($\sqrt{MSAE_B}$) of SVS versus SNR at various d and D for three scenarios. From Fig.1(a), the $\sqrt{MSAE_B}$ at $d = 0.05$ is less than that at $d = 0.15$ for $D = \lambda/2$. The reason is that the normal velocity component is zero but the pressure and in-plane velocity components are double their values in free-space if $d = 0$ and $D = \lambda/2$ for all $\theta_i = \pi/2$. Whereas, the normal velocity component is double their values in free-space but the pressure and in-plane velocity components are zero if $d = \lambda/4$ and $D = \lambda/2$ for all $\theta_i = \pi/2$. This situation results in the low signal problem. Thus, the d should be selected as close to 0. From Fig.1(b), the $\sqrt{MSAE_B}$ at $d = 0.15$ is less than that at $d = 0.05$ for $D = \lambda/2$. The reason is that the normal velocity component is double their values in free-space but the pressure and in-plane velocity components are zero at $d = 0$ and $D = \lambda/2$ for all $\theta_i = \pi/2$. Whereas, the normal velocity component is zero but the pressure and in-plane velocity components are double their values in free-space if $d = \lambda/4$ and $D = \lambda/2$ for all $\theta_i = \pi/2$. Thus, the d should be selected as close to $\lambda/4$, but the large d will increase the vessel's profile, which is undesirable. From Fig.1(c), the $\sqrt{MSAE_B}$ at $d = 0$ is less than that at $d = 0.25$ for $D = \lambda/2$. This is similar to result in rigid boundary. Since the overall array's spatial aperture at $D = \lambda/2$ is larger than that at $D = \lambda/4$, the $\sqrt{MSAE_B}$ at $D = \lambda/2$ is clearly less than that at $D = \lambda/4$ in three scenarios. When $D = \lambda/4$, however, the greater the d, the smaller the $\sqrt{MSAE_B}$ will be in three scenarios.

6. CONCLUSION

In this paper, a new spatial-vector smoothing algorithms for $multiple$ coherent sources is proposed based on the measurement model of 3-D cylindrical array with multi vector-hydrophones, which is located on or near a reflecting boundary. By summing the spatial covariance matrices from each "type" of component hydrophone, the rank up to 4 is restored without reduction of the array's geometric aperture, then by summing the spatial covariance matrices from each "ring" of cylindrical array, the rank up to $4P$ is restored. The performance of the proposed algorithm is examined in two practical applications: hull-mounted and seabed scenario. The $0 < d < \lambda/4$ and $D = \lambda/2$ should be selected to avoid rank lessen and increase estimating accuracy.

7. REFERENCES

[1] M. J. Berliner & J. F. Lindberg, *Acoustic Particle Velocity Sensors: Design, Performance and Applications*, Woodbury, New York, USA: AIP, 1996.

[2] A. B. Waite, *Sonar for practising Engineers*, 3rd edition, Chichester, Britain: Wiley, 2002.

[3] M. Hawkes & A. Nehorai, "Acoustic Vector-Sensor Processing in the Presence of a Reflecting Boundary," *IEEE Transactions on Signal Processing* vol. 48, no. 11, pp. 2981-2993, November 2000.

[4] T-J. Shan, M. Wax & T. Kailath, "On Spatial Smoothing for Direction-of-Arrival Estimation of Coherent Signals," *IEEE Transactions on Acoustics, Speech, Signal Processing*, vol. 33, pp. 809-811, August 1985.

[5] S. U. Pillai & B. H. Kwon, "Forward/Backward Spatial Smoothing Techniques for Coherent Signal Identification," *IEEE Transactions on Acoustics, Speech, Signal Processing*, vol. 37, pp. 8-15, January 1989.

[6] H. Wang & K. J. Ray Liu, "2-D Spatial Smoothing for Multipath Coherent Signal Separation," *IEEE Transactions on Aerospace & Electronic Systems*, vol. 34, pp. 391-405, April 1998.

[7] D. Rahamim, J. Tabrikian & R. Shavit, "Source Localization Using Vector Sensor Array in a Multipath Environment," *IEEE Transactions on Signal Processing*, vol. 52, pp. 3096-3103, November 2004.

[8] L. M. Brekhovskikh, *Waves in Layered Media*, 2nd ed. New York: Academic, 1980.

[9] A. Nehorai & E. Patan, "Acoustic Vector-Sensor Array Processing," *IEEE Transactions on Signal Processing*, vol. 42, pp. 2481-2491, Sept. 1994.

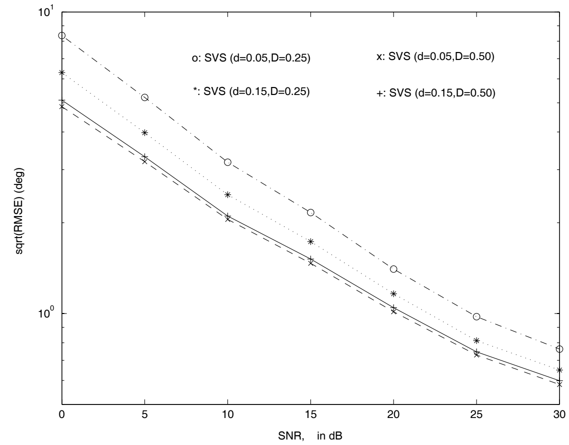

(a) in Rigid Boundary

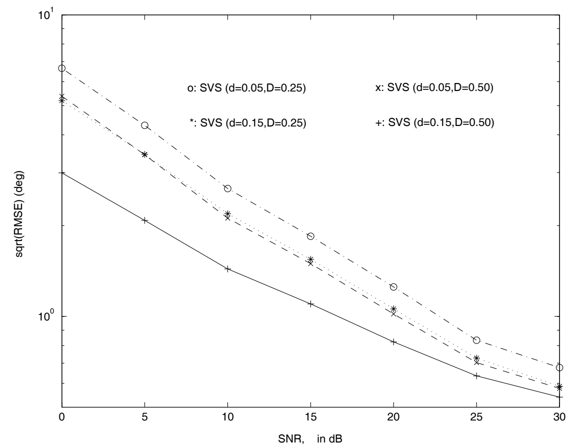

(b) in Pressure-Release Boundary

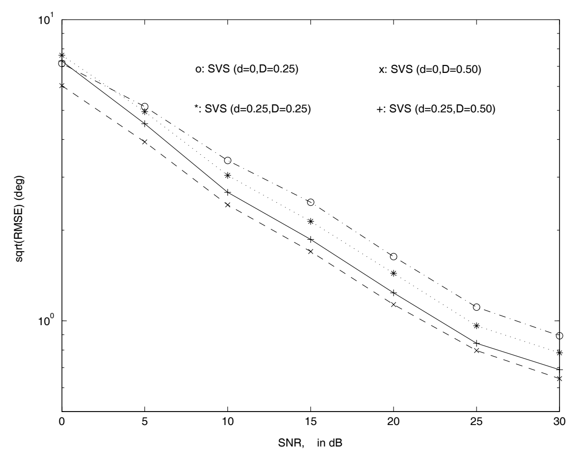

(c) in Seabed Model

Fig. 1. Performance ($\sqrt{MSAE_B}$) of SVS versus SNR: two equal-power narrowband, coherent sources with $\theta_1 = 50°, \phi_1 = 40°, g_1 = 1, \theta_2 = 20°, \phi_2 = 70°, g_2 = e^{j\pi/6}$ impinge upon a cylindrical array with eight vector-hydrophones